

Impact of Geometry and Feed Point on Radiation Pattern of a Patch Antenna and Its Linear Array as a Substitute of Multi-hop Link

Abu Sayed Md. Mostafizur Rahaman, Jesmin Akhter, Md.Imdadul Islam and M.R Amin, Member *IEEE*
Correspondence E-mail: *asmmr@juniv.edu*

Abstract— Rao-Wilton-Glisson (RWG) edge elements are widely used to determine the performance of an antenna specially the distribution of elemental dipole on the antenna surface, surface current distribution, profile of input impedance and radiation pattern. In this paper the impact of geometry and position of feed point of a patch antenna is analyzed in terms of variation of input impedance against frequency to get the bandwidth of the antenna and radiation pattern on both two dimensional surface and three dimensional space. Finally an array of such antenna is placed on a line to observe the end fire and broad side radiation pattern to get intense and heavily directed beam, can be used as substitute of multi hop ad-hoc link.

Index Terms— Security, In-polar and cross polar component, Green function, incident EM signal, impedance matrix and array antenna.

I. INTRODUCTION

DISTRIBUTION of surface current on the body of an antenna in receiving mode and the radiation pattern EM wave in transmitting mode is considered as the most important parameter in selection of antenna. In this paper we emphasis on patch antenna in context of above where the analysis is done based on RWG elements. The microstrip or patch antenna is widely used in in-door wireless communication for several reasons[1-3]: (a) the microstrip antenna is simple and inexpensive to manufacture (b) small in size therefore is compatible to be embedded inside handheld wireless communication devices (c) it can be mounted on rigid surfaces because of its stiffness in construction (d) supports both linear and circular polarization of EM wave. Although the directivity of a single antenna is poor but array of such antenna provides better directivity and gain.

The microstrip antenna can be considered as a segment of a planar transmission line usually used for indoor communications. The geometry of such antenna is shown in fig.1 where a metallic strip called patch and a ground plate are separated by a dielectric sheet of relative permittivity ϵ_r called substrate. The region above the upper plate of the antenna is air of dielectric ϵ_0 but the region below the upper plate is filled with medium of dielectric $\epsilon_0\epsilon_r$. Therefore the phase velocity of EM wave above and below the upper plate is different and the antenna cannot support TEM wave. For theoretical analysis the entire region above and below the upper plate is represented by an equivalent uniform transmission medium of dielectric [4-5],

$$\epsilon_{eff} = \frac{\epsilon_r + 1}{2} + \frac{\epsilon_r - 1}{2} \left\{ 1 + 12 \frac{h}{w} \right\}^{-1/2} \quad (1)$$

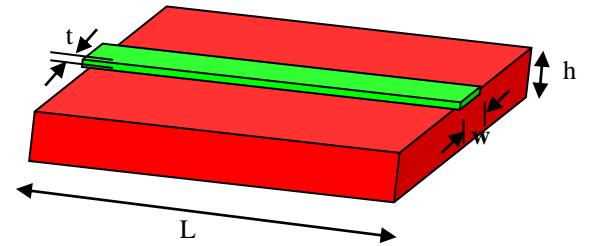


Fig.1. Basic patch antenna

The most widely used shape of patch antennas are square, circular, elliptical, rectangular, triangular and diamond. In this paper we considered only rectangular and circular patch. Feeding in patch antenna is achieved either by microstrip or co-axial line.

The electric and magnetic field in TM mode within the cavity is expressed as [6-8],

$$E_x = -j \frac{1}{\omega\mu\epsilon} \left(\frac{\delta^2}{\delta x^2} + k^2 \right) A_x; H_x = 0 \quad (2)$$

$$E_y = -j \frac{1}{\omega\mu\epsilon} \frac{\delta^2 A_x}{\delta x \delta y} \quad H_y = -\frac{1}{\mu} \frac{\delta A_x}{\delta z} \quad (3)$$

$$E_z = -j \frac{1}{\omega\mu\epsilon} \frac{\delta^2 A_x}{\delta x \delta z} \quad H_z = -\frac{1}{\mu} \frac{\delta A_x}{\delta y} \quad (4)$$

;where A_x is the vector magnetic potential obtained from the solution of homogeneous wave equation, $\nabla^2 A_x + k^2 A_x = 0$ and the boundary condition on the geometry of the antenna. We are more interested about the electric field outside of the antenna i.e. the radiation pattern of the antenna. The radiating field of the antenna is expressed as,

$$E_\phi^t = j \frac{k_0 h W E_0 e^{-jk_0 r}}{\pi r} \left\{ \sin \theta \frac{\sin(X)}{X} \frac{\sin(Z)}{Z} \right\} \cos \left(\frac{k_0 L_e}{2} \sin \theta \sin \phi \right) \quad (5)$$

; where $X = \frac{k_0 h}{2} \sin \theta \cos \phi$ and $Z = \frac{k_0 W}{2} \cos \theta$, $V_0 = hE_0$ is

the voltage across the slot, L_e is the effective length of the antenna.

The patch antenna behaves more like a cavity than a radiator so efficiency of such antenna is very poor but the efficiency can be enhanced by using it in an array. In this paper, the concept of RWG edge elements of [9-10] has been explored to determine distribution of RWG elements, profile of input impedance, and radiation pattern of a patch antenna. Entire work is done changing geometry of the patch and the feed points and combining them in a linear array. In a small indoor network or in ad-hoc network the access point can use array of microstrip antenna to enhance coverage in a certain direction or can provide single link access to the Base Station instead of multi-hop ad-hoc connection.

The organization of the paper is like: section-II reveals the entire mathematical analysis of evaluation of impedance matrix based on RWG edge elements, section-III depicts the results based on analysis of previous section and section-IV concludes the entire analysis.

II. SYSTEM MODEL

A. RWG Elements

An antenna in receiving mode experiences the rate of change of EM wave on its surface hence voltage is induced on the antenna by transformer action. The distribution of potential on the surface of the antenna is analyzed by RWG elements. Each RWG element is a pair of adjacent triangle symbolically represented as T_m^+ and T_m^- share common edge l_m having areas A_m^+ and A_m^- [10-11]. The RWG edge element of a thin dipole of antenna is shown in fig.2.

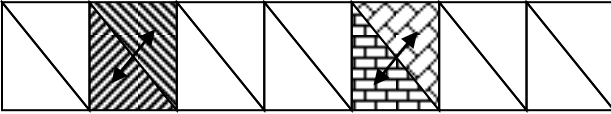


Fig.2. RWG edge elements on a thin dipole antenna

Fig.3 depicts the RWG element in details where parameters are:

- V_m^+ is the free vertex point of triangle T_m^+ ,
- V_m^- is the free vertex point of triangle T_m^- ,
- \mathbf{r}_m^{C+} is the free centroid point of triangle T_m^+ ,
- \mathbf{r}_m^{C-} is the free centroid point of triangle T_m^-
- $\rho_m^{C\pm}$ are the vectors between the free vector point

V_m^+ and the continued point $\mathbf{r}_m^{C\pm}$.

Here, $\rho_m^{C+} = \mathbf{r}_m^{C+} - V_m^+$ and $\rho_m^{C-} = \mathbf{r}_m^{C-} - V_m^-$.

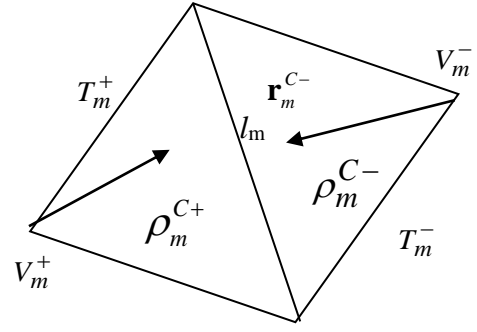


Fig.3. Close view of m-th RWG element

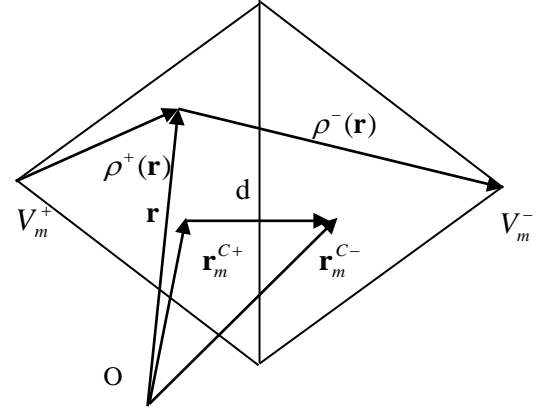


Fig.4. Observation Point on m-th RWG element

Fig.4 deals with a reference point O from which the distances of the centroids are: \mathbf{r}_m^{C+} and \mathbf{r}_m^{C-} ; that of the observation point is \mathbf{r} ; the distances between the observation point and the free vertices are $\rho^+(\mathbf{r})$ and $\rho^-(\mathbf{r})$ respectively. The length of the dipole, is $d = |\mathbf{r}_m^{C-} - \mathbf{r}_m^{C+}|$.

Let us start with the Helmholtz wave equation, $\nabla^2 A + k^2 A = -\mu j$, where the source is $-\mu j$ and A is the vector magnetic potential [12]. The solution of the equation is Green function can be written as [13, 14],

$$g_m^\pm(\mathbf{r}') = \frac{e^{-jk(\mathbf{r}_m^{C\pm} - \mathbf{r}')}}{|\mathbf{r}_m^{C\pm} - \mathbf{r}'|} \quad (6)$$

Let us define two integrals,

$$I_{mm}^+ = \int_{T_m^+} \rho_n^+(\mathbf{r}') g_m^+(\mathbf{r}') ds' \quad (7)$$

$$I_{mm}^- = \int_{T_m^-} \rho_n^-(\mathbf{r}') g_m^-(\mathbf{r}') ds' \quad (8)$$

Equations (7) and (8) can be compactly written as

$$I_{mm}^\pm = \int_{T_m^\pm} \rho_n^\pm(\mathbf{r}') g_m^\pm(\mathbf{r}') ds' \quad (9)$$

; Where, the observation point is on T_n^+ triangle.

Similarly,

$$J_{mm}^\pm = \int_{T_m^\pm} \rho_n^\pm(\mathbf{r}') g_m^\pm(\mathbf{r}') ds' \quad (10)$$

Where, the observation point is on T_n^- triangle.

Now, The vector magnetic potential,

$$A_{mn}^{\pm} = \frac{\mu l_n}{8\pi} \left[\frac{I_{mn}^{\pm}}{A_n^+} + \frac{J_{mn}^{\pm}}{A_n^-} \right] \quad (11)$$

Where, A_n^+ and A_n^- are respectively the areas of T_n^+ and

T_n^- .

Again the scalar potential,

$$\varphi_{mn}^{\pm} = \frac{1}{4\pi j\omega\epsilon} \left[\frac{l_n}{A_n^+} \int_{T_n^+} g_m^{\pm}(\mathbf{r}') ds' - \frac{l_n}{A_n^-} \int_{T_n^-} g_m^{\pm}(\mathbf{r}') ds' \right] \quad (12)$$

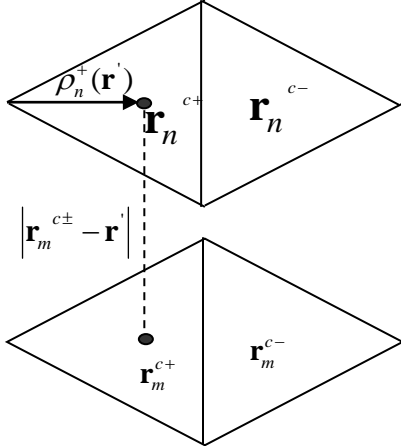


Fig.5. The m -th and n -th RWG elements

So, Impedance Z_{mn} correspond two edges elements m and n are

$$Z_{mn} = \ln \left[j\omega \left(\frac{A_{mn}^+ \cdot \rho_m^{c+}}{2} + \frac{A_{mn}^- \cdot \rho_m^{c-}}{2} \right) + \varphi_{mn}^+ - \varphi_{mn}^- \right] \quad (13)$$

Where, (\cdot) denotes the dot product.

Integration in (12) can be done in short for triangle T_m of fig.6 as

$$\int_{T_m} g_m^{\pm}(\mathbf{r}') ds' \approx A_m g(\mathbf{r}_m^c) \quad (14)$$

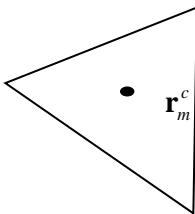


Fig.6. A single T_m triangle

Let E^{inc} is the electric field of an incident EM signal. In fig.7, electric field is in x -direction. Therefore, $E^{inc} = [E_x, 0, 0]$;

where $E_x = 1 \times e^{-jkz}$; $k = 2\pi/\lambda = \omega/c$. If the plate is located at $Z = 0$ then $E^{inc} = [1, 0, 0]$ V/m is the polarization of the plane wave. Now the voltage vector

$V_m = l_m [E_m^+ \cdot \rho_m^{c+} / 2 + E_m^- \cdot \rho_m^{c-} / 2]$ where $E_m^{\pm} = E^{inc}(\mathbf{r}_m^{\pm})$ and

$$E_m^{\mp} = [1 \times e^{-jkr_m^{c\pm}}, 0, 0] \quad V/m \quad (15)$$

Where, $m = 1, 2, 3, \dots, M$.

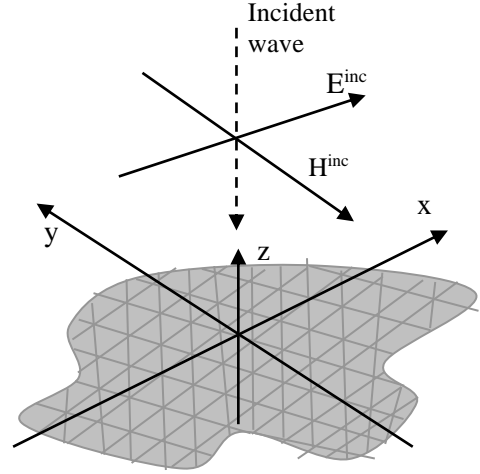


Fig.7. Incident field geometry for the patch

Now the moment equation $\mathbf{Z} \cdot \mathbf{I} = \mathbf{V}$, where \mathbf{Z} is an $M \times M$ impedance matrix and \mathbf{V} is the voltage vector with dimension $\mathbf{M} \times 1$ and $\mathbf{I} = [I_1, I_2, I_3, \dots, I_M]^T$, is the $\mathbf{M} \times 1$ current coefficient vector, where T represents transpose.

Now, the surface current diversity J_K for a given triangle k is obtained as

$$J_K = \sum_{m=1}^M I_m f_m(\mathbf{r}) \quad (16)$$

;where \mathbf{r} is an observation point in T_k and the basis function as [13-14]:

$$f_m(\mathbf{r}) = \begin{cases} \frac{l_m}{2A_m^+} \rho_m^+(\mathbf{r}); & \mathbf{r} \text{ in } T_m^+ \\ \frac{l_m}{2A_m^-} \rho_m^-(\mathbf{r}); & \mathbf{r} \text{ in } T_m^- \\ 0; & \text{Otherwise} \end{cases} \quad (17)$$

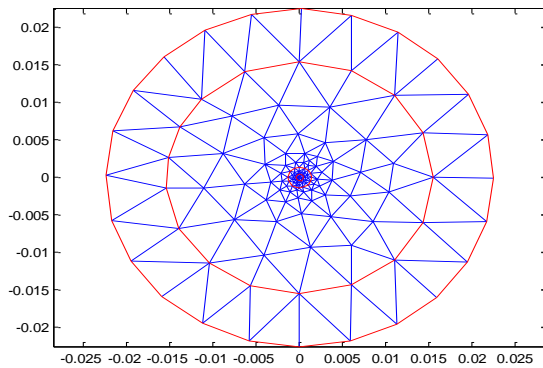
The entire analysis of this section is simulated using MATLAB 2013 and the corresponding result is shown in next section.

III. RESULTS

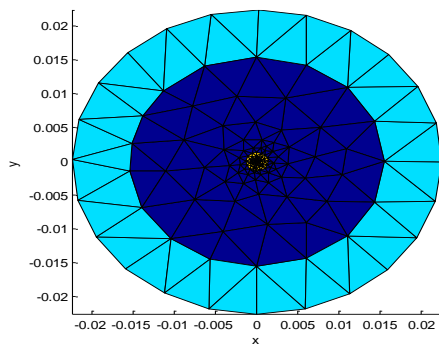
Fig. 8(a) shows the top view of distribution of rwg elements of a circular patch antenna. The same figure is also shown in 8(b) in a different form to distinguish the microstrip and the ground plate. Here the feed point is at the center of the patch. Fig. 9(a) shows the 3D view of the patch antenna along with the distribution of the rwg elements where the fig. 9(b) includes the dielectric material. The dimensions of the antennas are visualized from the fig. 8 and 9. The profile of

resistance and reactance of the antenna is shown in fig. 10. The resistance attains at its peak value at 2.3GHz and the reactance reaches at the peak value at 2.25GHz. The behavior of the impedance of the antenna is almost like a bandpass filter. Finally fig.11 shows the 2D and 3D radiation pattern of the antenna. The smaller circle of the fig. 11(a) indicates the radiation pattern of the cross-polar component and the outer circle indicates that of co-polar component. The directivity of the ‘in-plane electric field component’ is called the co-polar directivity that of the ‘out-of-plane electric field component’ is called the cross-polar directivity. The small circle on 2D radiation pattern is the cross-polar component and the larger circle is the co-polar radiation pattern. Both the radiation pattern is omni-directional.

Let us now shift the feed point at one corner keeping the geometry of the antenna like before. The corresponding 2D and 3D distribution of RWG elements are shown in fig. 12 and 13 respectively. Now the peak amplitude of the resistance and reactance is shifted at 2.375GHz and 2.3GHz respectively shown in fig.14. The radiation pattern of in-polar and cross-polar components are shown in fig.15. (a). Instead of omni-directional now the radiation pattern of co-polar component becomes directional but still the cross polar component remains omni-directional but its coverage is reduced.

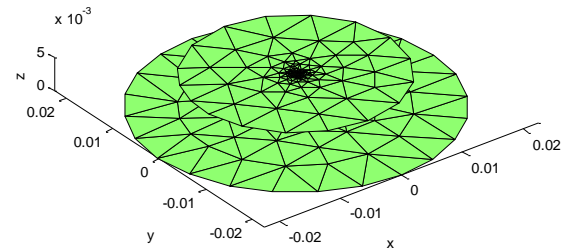


8(a)

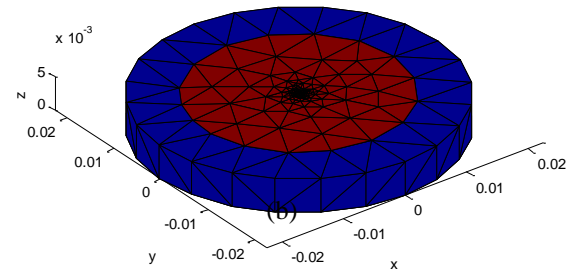


8(b)

Fig.8. Surface mesh of patch antenna (circular patch with feed at the center)



4(a)



4(b)

Fig.9. Volume mesh of patch antenna

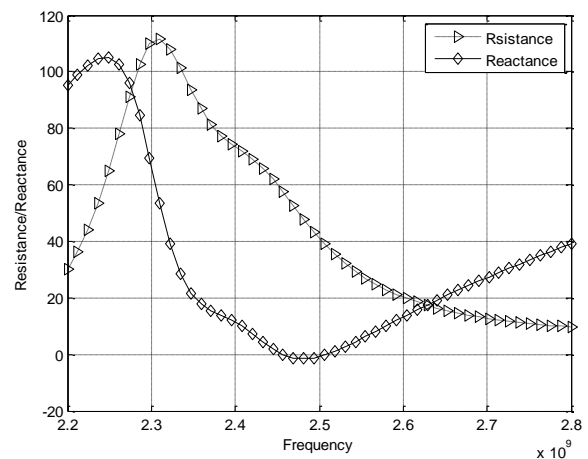
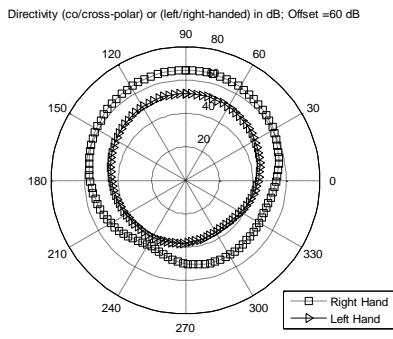
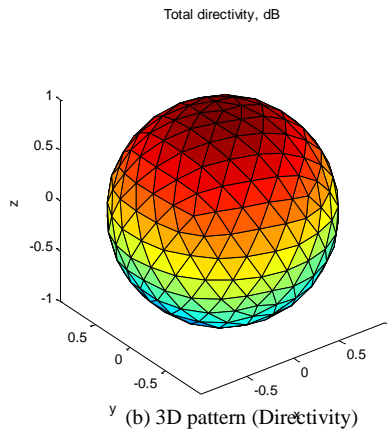


Fig.10. Profile of impedance of patch antenna

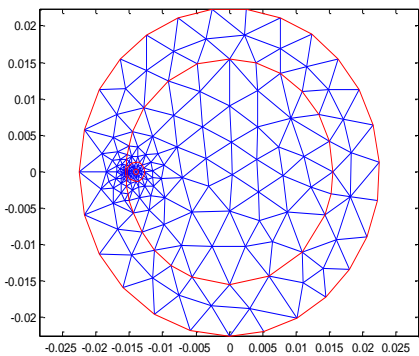


(a) E- plane

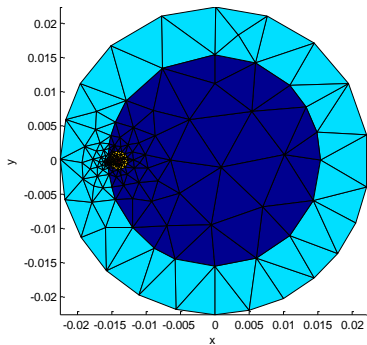


(b) 3D pattern (Directivity)

Fig.11. Radiation pattern of patch antenna (Circular shape with feed at the center)

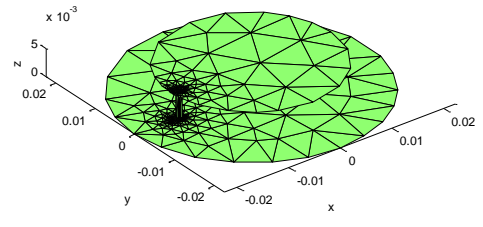


7(a)

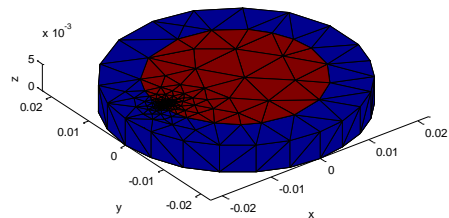


(b)

Fig.12. Surface mesh of patch antenna (circular patch with feed at one corner)



(a)



(b)

Fig.13. Volume mesh of patch antenna

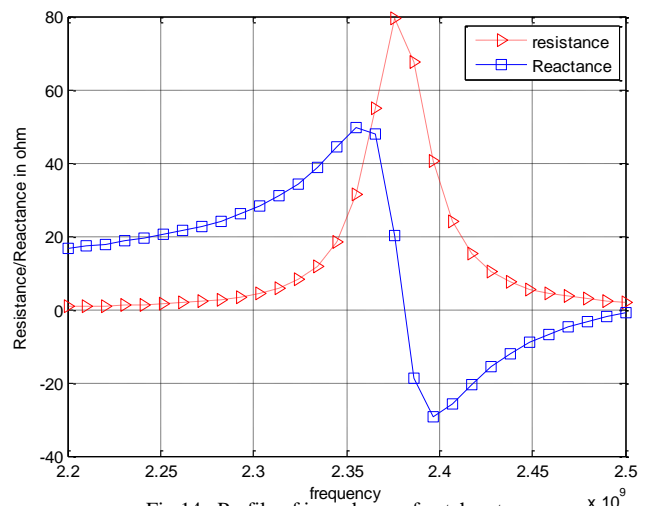
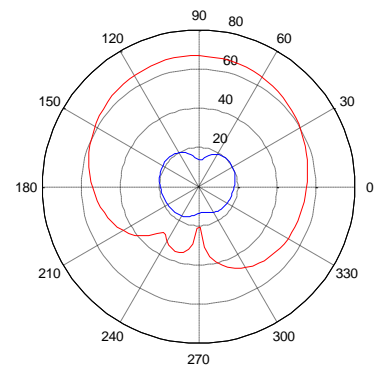
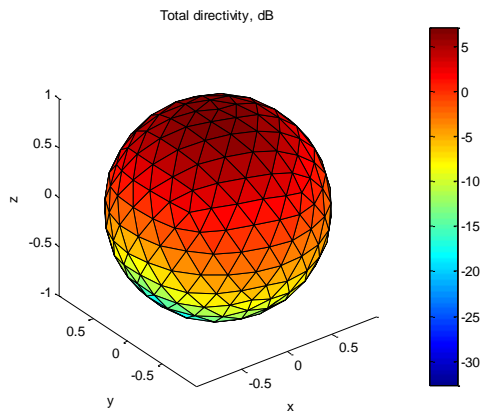


Fig.14. Profile of impedance of patch antenna

Directivity (co/cross-polar) or (left/right-handed) in dB; Offset =60 dB



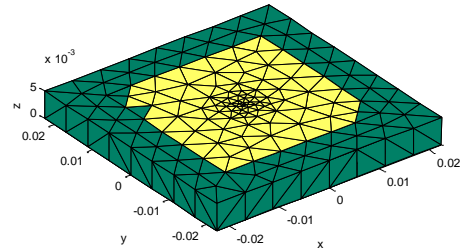
(a) E-plane plane



(b) 3D pattern (Directivity)

Fig.15. Radiation pattern of patch antenna (Circular shape with feed at one corner)

Next we used rectangular patch antenna of center feed whose RWG pattern is shown in fig.16 and 17 (both side view and top view). The peak amplitude of resistance and reactance (fig.18) are found almost at the same frequency like the case of circular patch. The radiation pattern of in-polar component is directional but that of cross polar component remains omnidirectional but its coverage is reduced like edge feed case of circular patch shown in fig.19. For the case of edge feed of rectangular patch, the RWG components and the impedance profile are shown in fig. 20, 21 and 22. Finally the radiation pattern of in-polar component and cross polar component both are found directional but the coverage of cross polar component is reduced shown in fig.23.



(b)

Fig.17. Volume mesh of patch antenna

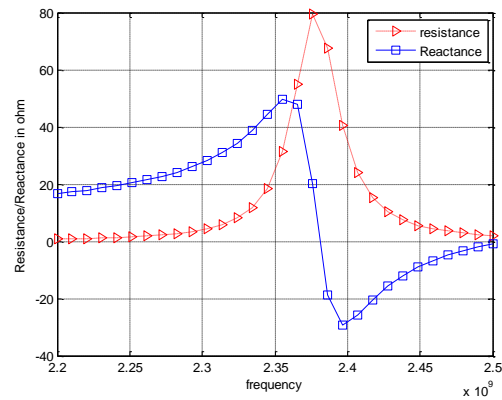


Fig.18. Profile of impedance of patch antenna

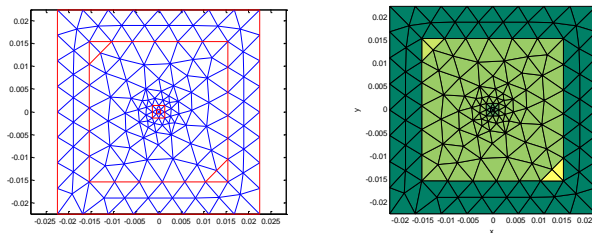


Fig.16. Surface mesh of patch antenna (rectangular patch with feed at the center)

Directivity (co/cross-polar) or (left/right-handed) in dB; Offset =60 dB

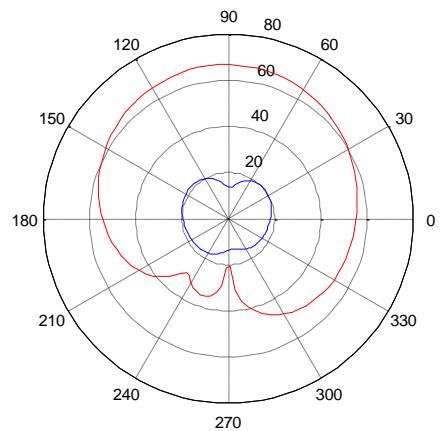
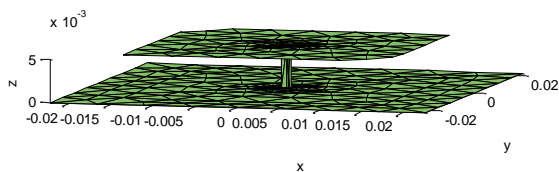


Fig.19. Radiation pattern of patch antenna on E-plane (rectangular shape with feed at the center)



(a)

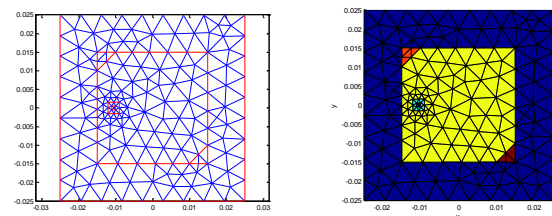
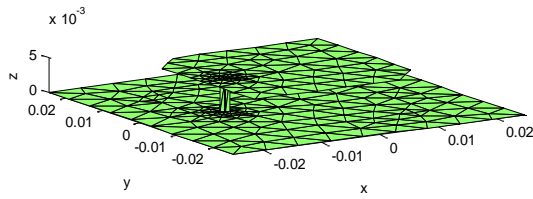
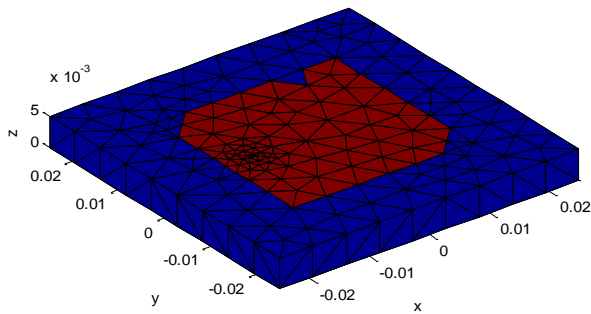


Fig.20. Surface mesh of patch antenna (rectangular patch with feed at one corner)



(a)



(b)

Fig.21. Volume mesh of patch antenna

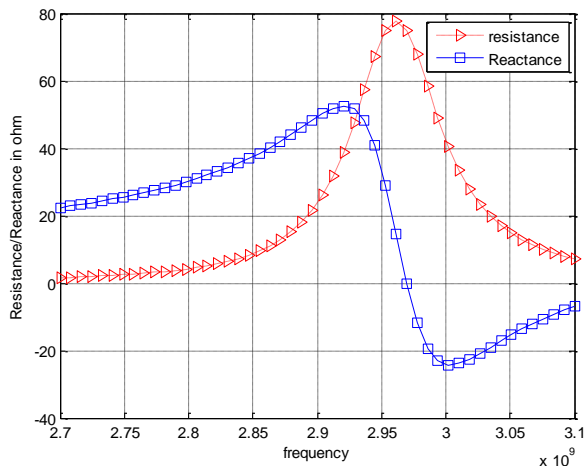


Fig.22. Profile of impedance of patch antenna

Directivity (co/cross-polar) or (left/right-handed) in dB; Offset =60 dB

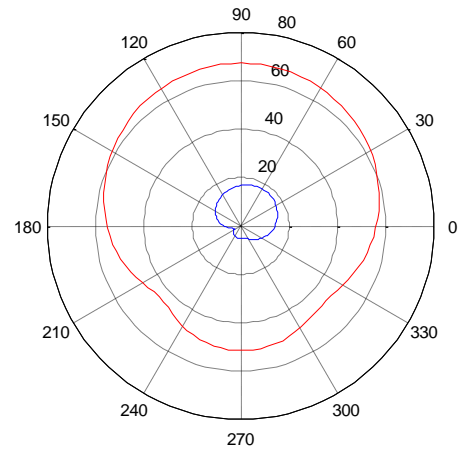


Fig.23. Radiation pattern of patch antenna on E-plane (rectangular shape with feed at one corner)

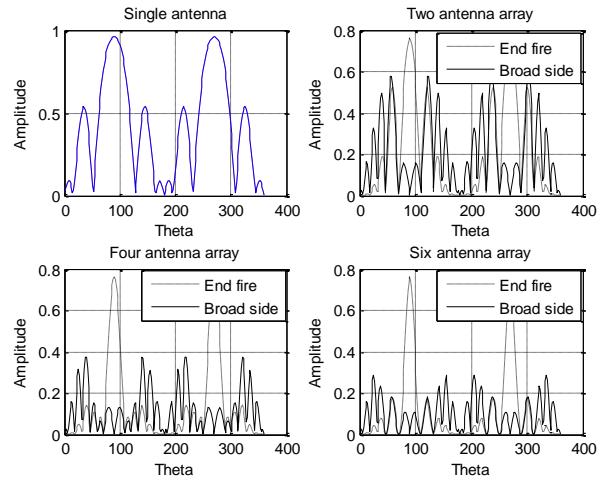


Fig.24. Radiation pattern of patch array

Finally the radiation pattern of a rectangular patch antenna with dimension of, $\lambda = 12\text{cm}$, $L_e = \lambda/2$, $h = 1\text{cm}$ and $w = \lambda/8$ is taken considering single antenna and linear array with separation of $d = \lambda/2$. Here both end-fire and broadside array is considered for 2, 4 and 6 antenna case and the corresponding radiation pattern is shown in fig. 24. It is visualized that patch antenna is more successful for end fire configuration since directivity becomes sharp and intensity of electric field is found high.

IV. CONCLUSION

The paper compares the performance of rectangular and circular patch antenna changing the position of feed point taking input impedance and radiation pattern as parameters. The result of the paper reveals that for circular strip case the radiation pattern of both co-polar and cross-polar component are omni directional when the feed point is at the center. When the feed point is moved at one corner the co-polar component becomes directional but still the cross-polar component remains omni directional. In case of rectangular strip both the components are approximately omni when the feed point is at

the center. For the case of corner feed point both the components become directional. Again for both circular and rectangular patch cases the peak value of resistance and reactance is shifted at higher frequency when the feed point is at the corner. Finally the weak radiation of the antenna is strengthened and made more direction using linear array. The analysis of the paper will be helpful for a wireless network planner to choose the optimum antenna for coverage of a small network.

REFERENCES

- [1] C. K. Aanandan, P. Mohanan, And K. G. Nair 'Broad-Band Gap Coupled Microstrip Antenna,' *IEEE Transactions on Antennas And Propagation*, vol.38, no.10, pp.1581-1586, OCTOBER 1990
- [2] M. H. Diallo Yaccoub, Achraf Jaoujal, Mohammed Younsi, Ahmed El Moussaoui, and Noura Aknin, 'Rectangular Ring Microstrip Patch Antenna for Ultra-wide Band Applications,' *International Journal of Innovation and Applied Studies*, Vol. 4 No. 2, pp. 441-446, Oct. 2013
- [3] Z.N. Chen, and M.Y.W Chia, 'Center-Fed Microstrip Patch Antenna,' *IEEE Transactions on Antennas and Propagation*, vol. 51, no. 3, pp. 483 – 487, March 2003
- [4] Md. Tanvir Ishtaique-ul Huque, Md. Kamal Hosain, Md. Shihabul Islam and Md. Al Amin Chowdhury, 'Design and Performance Analysis of Microstrip Array Antennas with Optimum Parameters for X-band Applications,' (*IJACSA*) *International Journal of Advanced Computer Science and Applications*, pp.81-87, Vol. 2, No. 4, 2011
- [5] Mahdi Ali, Abdennacer Kachouri and Mounir Samet, 'Novel Method for Planar Microstrip Antenna Matching Impedance,' *Journal of Telecommunications*, vol.2, ISSUE-2, pp.131-138, May 2010
- [6] C.A. Balanis. "Antenna Theory: Analysis and Design", 2nd Ed, Wiley, New York, 1997
- [7] Kraus, J. D. (1988), *Antennas*, McGraw-Hill, New York.
- [8] D. M. Pozar, *Microwave Engineering*, Wiley, New York, 2005, third edition
- [9] S.M. Rao, D.R. Wilton, and A.W. Glisson, 'Electromagnetic Scattering by Surfaces of Arbitrary Shape', *IEEE Trans. Antennas and Propagation*. Vol. 30 (3): pp. 409-418, 1982.
- [10] Sergey N. Markarov, 'Antenna & EM Modeling with MATLAB,' Wiley-Interscience, 2003, USA
- [11] S. Makarov, 'Mom Antenna Simulations, with Matlab: RWG Basis Functions,' *IEEE Trans. Antennas and Propagation*, vol. AP-43, no. 5, pp. 100-107, October 2001.
- [12] Md. Asif Hossain¹, Mushlah Uddin Sarkar, M.R. Amin and Md. Imdadul Islam, 'Performance Comparison of Bow-Tie and Slot Antenna Based on RWG Edge Elements,' Second International Conference on Computer Research and Development, *IEEE Computer Society*, pp.839-843, 2010
- [13] Mushlah Uddin Sarkar, Md. Asif Hossain¹, M.R. Amin and Md. Imdadul Islam, 'The Impact of Frequency on Radiation Pattern of Bowtie and Spiral Antenna Based on RWG Elements,' *2010 2nd International Conference on Electronic Computer Technology (ICECT 2010)*, pp.137-141, 2010
- [14] Abu Sayed Md. Mostafizur Rahaman, Jesmin Akhter and Md. Imdadul Islam, 'Array Antenna System of Frequency Independent Antennas Based on RWG Elements,' *Journal of Electronics and Computer Science Research*, vol. 2 no.1, pp.7-14, April 2013



Abu Sayed Md. Mostafizur Rahaman received his M.Sc. degree from Stuttgart University at Stuttgart, Germany in Information Technology (INFOTECH) in the branch of Embedded System Engineering in 2009. He received his B.Sc. degree in Electronics and Computer Science, from Jahangirnagar University, Savar, Dhaka, Bangladesh in 2003. Since 2004, he is a faculty member having current Designation "Associate Professor" in the Department of Computer Science and Engineering of Jahangirnagar University, Savar, Dhaka, Bangladesh. During his graduation, he worked at BOSCH (biggest automobile company in Germany) as Trainee engineer (Industrial internship) as part of his graduate degree in embedded Systems. Currently his research focuses on telecommunication, Embedded and Parallel Systems, Reconfigurable Computing, Multicore Architecture and Software Engineering. Now he is pursuing PhD at the Department of Computer Science and Engineering, Jahangirnagar University, Dhaka, Bangladesh in the field of Multipath Fading effect in Wireless Communication.



Jesmin Akhter received her B.Sc. Engineering degree in Computer Science and Engineering from Jahangirnagar University, Savar, Dhaka, Bangladesh in 2004 and M.Sc Engineering degree in Computer Science and Engineering from Jahangirnagar University, Savar, Dhaka, Bangladesh in 2012. Since 2008, she is a faculty member having current Designation "Assistant Professor" at the Institute of Information Technology in Jahangirnagar University, Savar, Dhaka, Bangladesh. Her research areas are on network traffic, complexity and algorithms and software engineering. Now she is pursuing PhD at the Department of Computer Science and Engineering, Jahangirnagar University, Dhaka, Bangladesh in the field of 4G wireless networks.



Md. Imdadul Islam has completed his B.Sc. and M.Sc Engineering in Electrical and Electronic Engineering from Bangladesh University of Engineering and Technology, Dhaka, Bangladesh in 1993 and 1998 respectively and has completed his Ph.D degree from the Department of Computer Science and Engineering, Jahangirnagar University, Dhaka, Bangladesh in the field of network traffic engineering in 2010. He is now working as a Professor at the Department of Computer Science and Engineering, Jahangirnagar University, Savar, Dhaka, Bangladesh. Previously, he worked as an Assistant Engineer in Sheba Telecom (Pvt.) LTD (A joint venture company between Bangladesh and Malaysia, for Mobile cellular and WLL), from Sept.1994 to July 1996. Dr Islam has a very good field experience in installation of Radio Base Stations and Switching Centers for WLL. His research field is network traffic, wireless communications, wavelet transform, OFDMA, WCDMA, adaptive filter theory, ANFIS and array antenna systems. He has more than 150 research papers in national and international journals and conference proceedings.



M. R. Amin received his B.S. and M.S. degrees in Physics from Jahangirnagar University, Dhaka, Bangladesh in 1984 and 1986 respectively and his Ph.D. degree in Plasma Physics from the University of St. Andrews, U. K. in 1990. He is a Professor of Electronics and Communications Engineering at East West University, Dhaka, Bangladesh. He served as a Post-Doctoral Research Associate in Electrical Engineering at the University of Alberta, Canada, during 1991-1993. He was an Alexander von Humboldt Research Fellow at the Max-Planck Institute for Extraterrestrial Physics at Garching/Munich, Germany during 1997-1999. Dr. Amin was awarded the Commonwealth Postdoctoral Fellowship in 1997. Besides these, he has also received several awards for his research, including the Bangladesh Academy of Science Young Scientist Award for the year 1996 and the University Grants Commission Young Scientist Award for 1996. His current research fields are wireless communications and networks and also nonlinear plasma dynamics. He is a member of the IEEE.